Eng. & Technology, Vol.25, Suppl.of No.3, 2007

Design and Analysis of A 3-D Conical Diffuser

Dr. Arkan K. Husain Al Tai

Received on:27/11/2005
Accepted on:14/5/2006

Abstract:
Analysis of flow through the conical diffuser of an annular combustion system is presented. The flow is assumed to be unsteady, quasi three dimensional, compressible and turbulent. A k-ε model was used to simulate turbulence. Several area ratios and divergence angles were tested until circulation took place. At this angle a snout was introduced to correct the flow. A control volume method was used to solve the differential equations of the flow to obtain velocity and pressure coefficient distributions. The numerical results show that the axial velocity decreases with diffuser length for a certain divergence angle. But it increases with angle of divergence for the same area ratio, while the radial component of velocity was found to increase with both. It was proved that the snout can correct the flow whenever circulation takes place.

key words: combustors, diffusers, snout

الخلاصة
يتم استعراض تحليل الجريان خلال ناشر مخروطي لغرفة احتراق طوقية. تم افتراض الجريان غير مستقر، مقرب الى ثلاثي الابعاد، انضغاطي و مظطرب. تم استخدام نموذج (k - ε) للاظطراب. تم تجربة العديد من نسب المساحة و زوايا الانفراج وحتى حصول الدوران. عند هذه الزاوية تم استخدام (سنوت) لتصحيح الجريان. استخدمت طريقة حجم السيطرة لحل المعادلات التفاضلية للجريان للحصول على توزيع السرعة ومعامل الضغط. ان النتائج تبين نقصان السرعة المحورية مع طول الناشر لزاوية انفراج معينة. ولكنها تزداد مع زاوية الانفراج لنسبة مساحة معينة. بينما مركبة السرعة الشعاعية وجدت انها تزداد مع الاثنين. وتم التحقق من ان استخدام ال (سنوت) يصحح الجريان اينما يحدث الدوران.
[كلمات مفاتيح: ناشر، غرف الاحتراق ، السنوت].

Symbols:

K turbulent kinetic energy. [kJ/kg]
U velocity in X-direction [m/s]
V velocity in r-direction [m/s]
P pressure [N/m^2]
S radiation term
β density term
Γ diffusion coefficient
ε rate of energy dissipation [W/kg]
Φ source term
Δx normalized dimension
Δr normalized dimension
μ viscosity [kg/m.s]
ρ density [kg/m^3]
σ Schmidt number [kg/m^3]
subscripts:

* Dept. of Technical Education, UOT., Baghdad-IRAQ.

https://doi.org/10.30684/etj.25.3.16
2412-0758/University of Technology-Iraq, Baghdad, Iraq

E, W, P,N, S	grid points
E, w, n, s	control volume faces
Nb	neighbors
t	turbulent
e	effective
ε	kinetic energy
k	dissipation rate

Introduction:

The flow exiting the compressor has a relatively high velocity. For flame stabilization purposes, this velocity has to be reduced. To do so a diffuser is incorporated ahead of the combustor. This is becoming an essential part of the combustion system. For flow stabilization purposes this diffuser should be as long as possible. But for mechanical considerations it should be as short as possible. Its length has become a tradeoff issue. However, to design a short diffuser, the angle of divergence should be large. This could be large enough to cause circulation of flow. This means incurring areas of an unacceptable loss of flow energy. One method to correct for this is to incorporate a snout in the diffuser. There are several types of diffusers, circular , or rectangular. Flow in the diffuser can be turbulent due to high Reynolds numbers and the adverse pressure gradients which cause early transition of laminar to turbulent away from separation condition. Flow in diffusers can generally be assumed as two dimensional. Incorporating a snout separation can further be delayed and can improve diffuser efficiency[1] .

A vortex controlled diffuser was described by Ringleh[2] , which relied solely on the aerodynamic design of cusps in the diffuser walls to locate vortices. The objective was to reduce the boundary shear stress experienced by the flow in the region of high adverse pressure gradients. This was to be achieved by replacing the fixed wall with a vortex rotating preferentially in the direction of flow. Only limited success was obtained due to the difficulty in retaining a stable vortex system, as energy was lost within the cusp by skin friction.

Weber [3] studied the swirling flow inside a conical diffuser. He derived the momentum integral equation from elementary portion of the boundary layer for both laminar and turbulent flows. For the laminar flow an appropriate velocity profile for u and v were assumed using Pablhausen method , where u and v are the velocity components in X and θ directions. The wall shear stresses were evaluated using the gradients of u and v in the direction normal to the wall. The momentum integral equations were finally put into a dimensionless form. The equation obtained was similar to that derived by Taylor[4] .

While for the turbulent flow, Weber used the one seventh power distribution of v_R and v_θ . The momentum equations was then solved numerically to obtain the boundary layer thickness and path of fluid particles on the surface of the cone.

Theoretical Analysis:

The flow in the diffuser is assumed to be unsteady, compressible and axi - symmetric. The continuity, momentum, and energy equations under these assumptions are[5]:

Continuity equation:

$$\partial\rho/\partial t + \partial(\rho u/\partial X + 1/r\ \partial(\rho vr)/\partial r = 0 \quad \ldots.(1)$$

X – Momentum equation:

$$\frac{\partial(ru)}{\partial t}+\frac{\partial}{\partial X}\left(\partial u^2\right)+\frac{1}{r}\frac{\partial}{\partial r}\left(r\partial vu\right) - \frac{\partial}{\partial X}\left(m\partial u/\partial X\right)-\frac{1}{r}\frac{\partial}{\partial r}\left(mr\partial u/\partial r\right)= -\frac{\partial r}{\partial X}+\frac{\partial}{\partial X}\left(m\partial u/\partial X\right)+\frac{1}{r}\frac{\partial}{\partial r}\left(mr\partial v/\partial X\right) \quad (2)$$

R – Momentum equation:

$$\frac{\partial(rv)}{\partial t}+\frac{\partial}{\partial X}\left(\partial uv\right)+\frac{1}{r}\frac{\partial}{\partial r}\left(r\partial v^2\right) - \frac{\partial}{\partial X}\left(m\partial v/\partial X\right)-\frac{1}{r}\frac{\partial}{\partial r}\left(mr\partial v/\partial r\right)= -\frac{\partial r}{\partial r}+\frac{\partial}{\partial X}\left(m\partial u/\partial X\right)+ \frac{1}{r}\frac{\partial}{\partial r}\left(mr\partial v/\partial r-2mv/r^2\right) \quad (3)$$

K – equation:

$$\frac{\partial(rk)}{\partial t}+\frac{\partial}{\partial X}\left(ruk\right)+\frac{1}{r}\frac{\partial}{\partial r}\left(rrvk\right) - \frac{\partial}{\partial X}\left(\Gamma_e\,\partial k/\partial X\right)-\frac{1}{r}\frac{\partial}{\partial r}\left(\Gamma r\partial k/\partial r\right)= \left(G_K-re\right) \quad (4)$$

ε- equation:

$$\frac{\partial(re)}{\partial t}+\frac{\partial}{\partial X}\left(\partial ue\right)+\frac{1}{r}\frac{\partial}{\partial r}\left(r\partial e\right) - \frac{\partial}{\partial X}\left(\Gamma\partial e/\partial X\right)-\frac{1}{r}\frac{\partial}{\partial r}\left(\Gamma_e r\partial e/\partial r\right)= \left(C1G_K-C_2re\right)\frac{e}{k} \quad (5)$$

G_k can be found from the equation:

$$G_k= \mu_t[2[(\partial u/\partial X)^2+(\partial v/\partial r)^2+(v/r)^2]+(\partial u/\partial r+\partial v/\partial x)^2]$$

where C_1 and C_2 are constants.

Γ_k and Γ_ε are the effective exchange coefficients for k and ε, respectively. They are given by:

$$\Gamma_{k\,eff} = \frac{\mu_{eff}}{\delta_{k\,eff}}$$

$$\Gamma_{\varepsilon\,eff} = \frac{\mu_{eff}}{\delta_{\varepsilon\,eff}}$$

$\Gamma_{k\,eff}$, and $\Gamma_{\varepsilon\,eff}$ are the effective Schmidt numbers when k and ε are assumed constants.

$\Gamma_{k\,eff}$ =0.9

$$\Gamma_{\varepsilon\,eff} = \frac{k^2}{(C_2-C_1)C_D^{1/2}}$$

where k =0.4 is the VonKarman constant.
C_1= 1.43, C_2= 1.92, C_D= 0.09

$$m_r=\frac{C_D rK^2}{e}\quad,\ \mu_{eff}=\mu_L+\mu_t$$

where:
μ_L is the laminar viscosity, and
μ_t is the turbulent viscosity.
The energy equation will be:

$$\frac{\partial(rh_0)}{\partial t}+\frac{\partial}{\partial X}(ruh_0)+\frac{1}{r}\frac{\partial}{\partial r}(rrXh_0)$$

$$-\frac{\partial}{\partial X}\left(\Gamma\Phi\frac{\partial\Phi}{\partial X}\right)-\frac{1}{r}\frac{\partial}{\partial r}\left(r\Gamma\frac{\partial\Phi}{\partial X}\right)=S_\Phi h_0 \ldots(7)$$

where: S_Φ =0 for no radiation.

Governing Differential Equations:

$$\frac{\partial(b\Phi)}{\partial t}+\frac{\partial}{\partial X}(bu\Phi)+\frac{1}{r}\frac{\partial}{\partial r}(rbv\Phi)-$$

$$\frac{\partial}{\partial X}\left(\Gamma_\Phi\frac{\partial\Phi}{\partial X}\right)-\frac{1}{r}\frac{\partial}{\partial r}\left(r\Gamma\frac{\partial\Phi}{\partial r}\right)=S_\Phi \ldots\ldots\ldots(8)$$

Continuity equation:

$\Phi = 1, \quad \beta = \rho, \quad \Gamma = 0, \quad S_\Phi = 0$

X – Momentum equation:

$\Phi = u, \quad \beta = \rho, \quad \Gamma = \mu$

$$S_\Phi=\frac{\partial}{\partial X}\left(m\frac{\partial u}{\partial X}\right)+\frac{1}{r}\frac{\partial}{\partial r}\left(rm\frac{\partial v}{\partial X}\right)$$

R – Momentum equation:

$\Gamma = \mu, \quad \beta = \rho, \quad \Phi = v$

$$S_\Phi=\frac{-\partial r}{\partial r}+\frac{\partial}{\partial X}\left(m\frac{\partial u}{\partial r}\right)+\frac{1}{r}\frac{\partial}{\partial r}\left(rm\frac{\partial v}{\partial r}\right)-\frac{2mv}{r^2}$$

K – equation:

$S_\Phi = G_k - \rho\varepsilon, \quad \beta = \rho, \quad \Phi = k$

$$\Gamma = \frac{\mu_{eff}}{\delta_{eff}}$$

ε - equation:

$$S_\Phi=(C_1G_k-C_2re)e/k$$

$$\Gamma = \frac{\mu_{eff}}{\delta_{eff}}$$

$\beta = \rho, \quad \Phi = \varepsilon$

h_0 - equation:

$S_\Phi = 0, \quad \Gamma = \frac{m}{d_{ho}}, \quad \beta = \rho,$

$\Phi = h_0$

The calculation domain was divided into a number of non- overlapping control volumes, such that there is one control volume surrounding each grid point, as shown in Figures (1), and (2).

The Calculation Algorithm:

The calculation procedure follows the following steps:

1- The finite difference coefficients for the x momentum equation no.2, are computed. The effective viscosity and the source term are obtained from appropriate physical laws and modules.
2- The finite difference form of the x-momentum equation no.2 is solved by TDMA traverses using an estimated pressure field. Thus obtaining the U^* field.
3- The finite difference coefficients for the R – momentum equation no.3 are computed. This is similar to step no.1.
4- The finite difference form of the R-momentum equation no.3 is solved by TDMA traverse, using the estimated pressure field. Thus the V^* velocity field is obtained.
5- The guessed velocity fields of steps 2 and 4 are used to compute sources in the pressure correction which are the solved by the TDMA

traverses. The resulting pressure corrections are used to correct the velocity and pressure fields.

6- Sectional balance adjustments are performed to satisfy strip wise continuity of the U-velocity field and of pressure. The V- velocity field is obtained from local continuity equation. This completes the solution of momentum and continuity equations.
7- For all other variables, the exchange coefficients and source terms are calculated from the K-turbulence model given in equations 4 and 5. the finite difference coefficients are calculated by solving the equations using TDMA traverses.
8- Sectional balance adjustments are made with pressure adjustments and the satisfaction of local continuity should be also ensured[6, 7, 8] .
9- These steps are repeated until convergence is obtained.
10- Once convergence is reached, then the energy equation can be solved.

Results and Discussion:

The equations of continuity, momentum, and energy were solved for axi symmetric flow using the control volume method. It was noticed that holding the inlet conditions, wall length, and throat area constant while, varying the divergence angle leads to the following flow regimes: for divergence angles 7^0, and 15^0 there are no appreciable stall as can be seen in Figures 3 and 4.

For divergence angle of 25^0, there were a large transitory stall as can be seen in Figure 5. The flow was separated from both walls. Separation started just downstream from the throat and reattach downstream the diffuser exit. The flow was corrected by a snout as can be seen in Figures 6 for axial velocity and 10 for the radial velocity.

Figures 3 and 4 show the distribution of the axial velocity U along the diffuser for an area ratio of 2.5. They show that for the same angle, the velocity decreases. But for shorter diffusers the velocity increases with angle of divergence.

Figure 6 shows the effect on flow when incorporating a snout in the diffuser. The flow well behaves and circulation has disappeared.

Figures 7, 8, and 9 show the distribution of the radial velocity component V along the diffuser. They show that V increases with both diffuser length and with divergence angle due to divergence increase. The values of V at the centre line stream are very small where U is maximum. Figure 9 also show the effect of the wall on the value of V.

Figure 10 shows the distribution of the velocity component V along the diffuser when a snout is incorporated. It shows that the flow is corrected.

Figures 11,12, and 13 show the pressure contours along the diffuser. They show that the pressure increase with length due to the reduction in velocity by diffusion while it decreases with angle of divergence. Figure 14 shows the pressure contours for a diffuser with snout. It shows a well behave flow. Figure 15 is a schematic drawing of an annular diffuser with snout [9].

Conclusions:

The following points can be concluded:

1. The diffuser divergence angle can be increased up to 25^0 without incurring sensed separation.
2. At the angle of 25^0 a large transitory stall occurs.
3. Incorporation of a snout has proved to be effective to remove the stall and correct the flow.
4. k–ε model has been used successfully to simulate turbulence.
5. The axial velocity was found to decrease with diffuser length and increase with divergence angle for the same area ratio.
6. The radial velocity component was found to increase with length and with divergence angle.

References:

1- Paul ,K. G., ”Separation of flow”, Pergammon press, first edition, 1970.

2- Ringleh, F. O., “Flow control by generation of standing vortices the cusp effects” , Aeronautical report No. 317, July 1955.

3- Weber, H. E., “ The boundary layer inside a conical surface due to swirl”, J. Applied Mech., December 1956.

4- Taylor, G. E., “The boundary layer in the converging nozzle of a swirl atomizer” , Quart. Mech. And applied math., V.3, p.2, 1950.

5- Hoffmann, Klausa, “Computational fluid dynamics for engineering”, Publication of engineering education system, USA, 1989.

6- Faraj, J. J., “ Effect of axial velocity distribution on performance of axial flow compressor cascade”, M. Sc. thesis, University of Baghdad, 1991.

7- Patankar, S. V., ”Numerical heat transfer and fluid flow”, Taylor Group, New York, 1980.

8- Versteeg H. K. , and Malalase K. W., “An introduction to computational fluid dynamics, the finite volume method”, Longman group Ltd., 1995.

9- Lefebvre A. H., “Gas turbine combustion”, McGraw Hill book company, London, 1983.

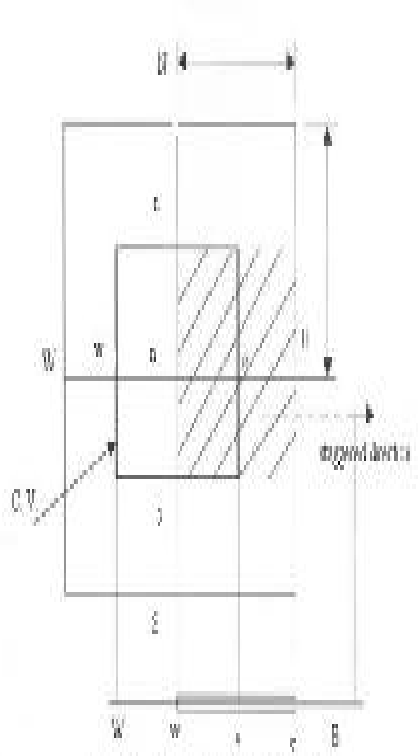

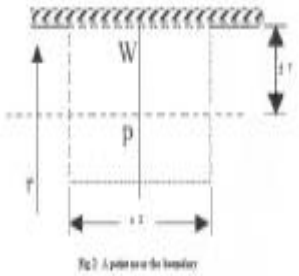

Fig. 2 A point near the Boundary

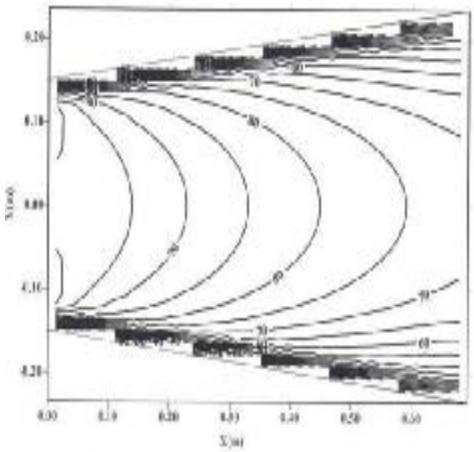

Fig.3 : Axial velocity contours
θ = 7 Degrees

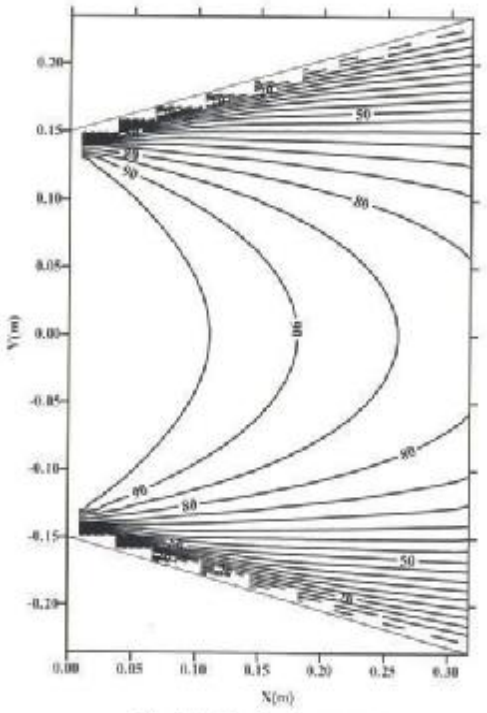

Fig.4 : Axial velocity contours
θ = 15 Degrees

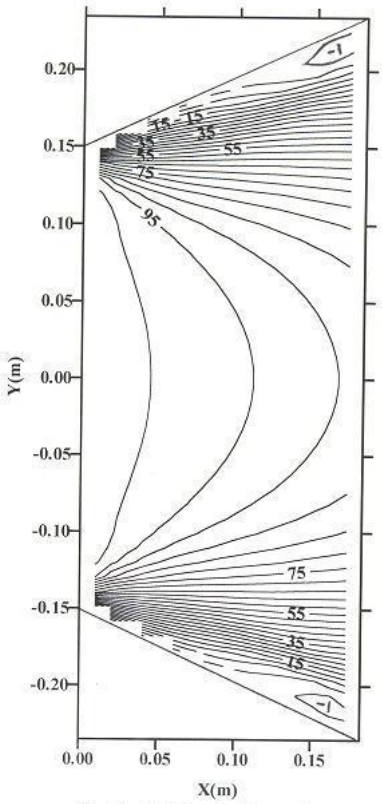

Fig. 5 : Axial velocity contours
θ = 25 Degrees

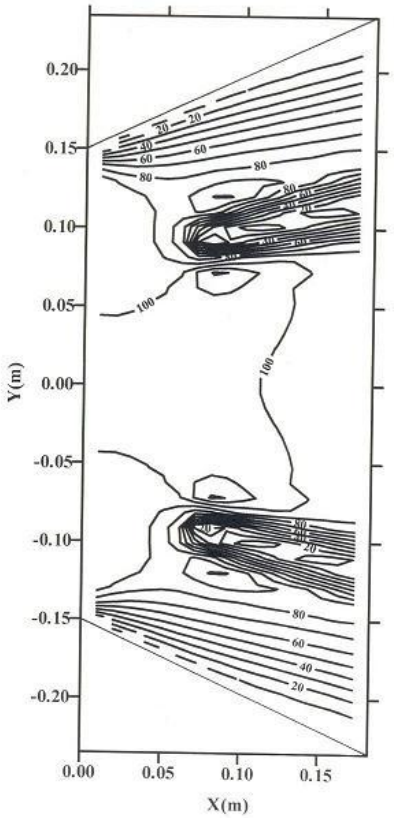

Fig. 6: Axial velocity contours
with snout (angle 25 degrees)

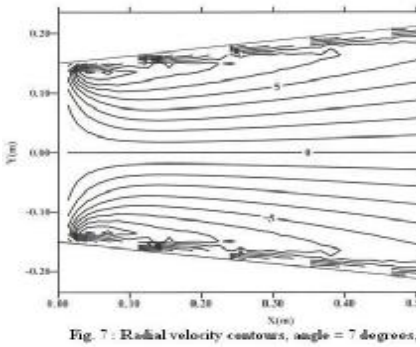

Fig. 7 : Radial velocity contours, angle = 7 degrees.

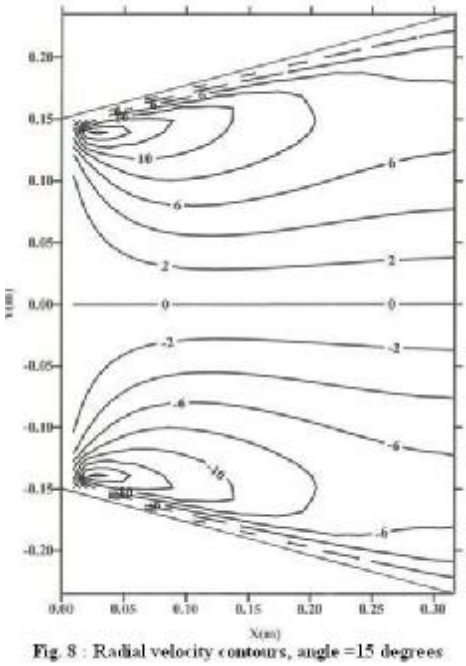

Fig. 8 : Radial velocity contours, angle =15 degrees

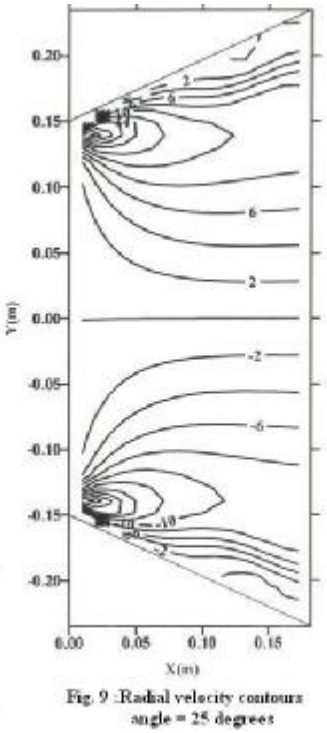

Fig. 9 :Radial velocity contours angle = 25 degrees

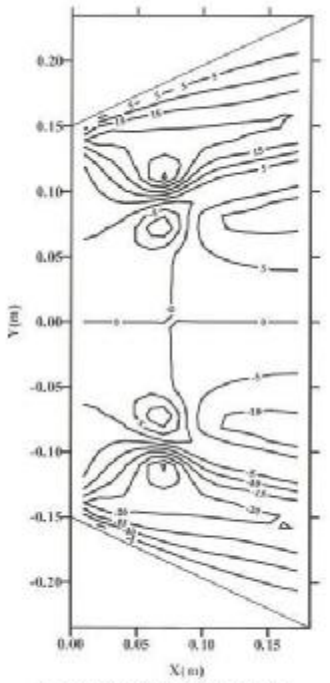

Fig. 10 : Radial velocity contours angle = 15 degrees, with inlet

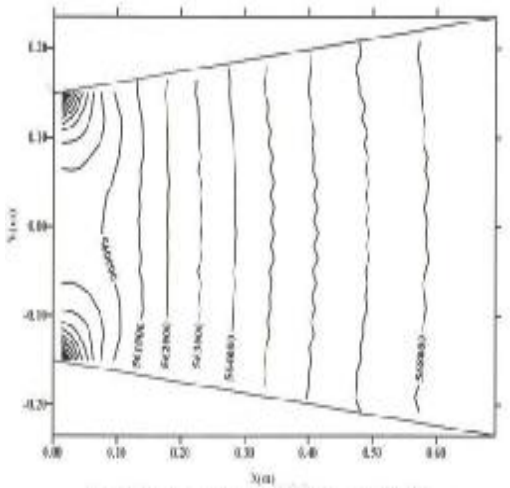

Fig. 11 : Pressure contours, angle = 7 degrees, AR = 1.5

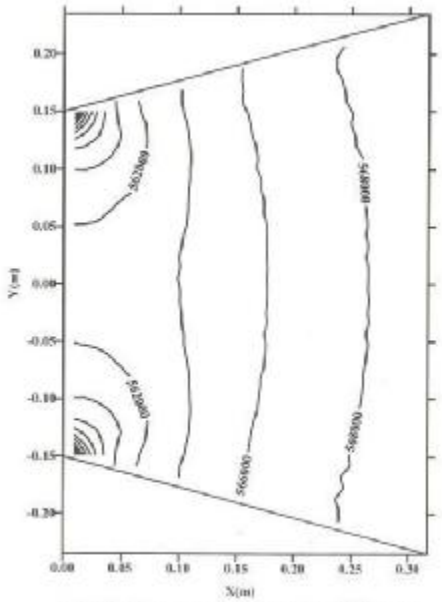

Fig. 12 : Pressure contours, angle = 15 degrees

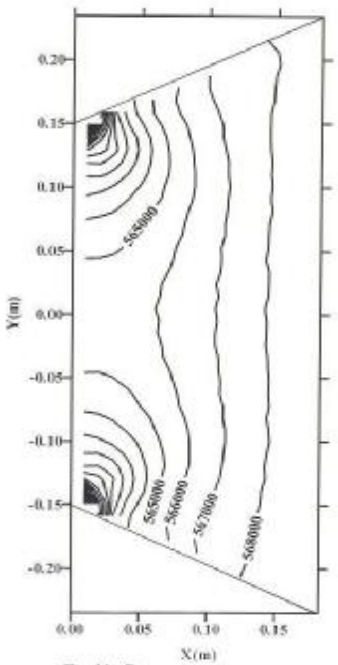

Fig. 13 : Pressure contours angle = 25 degrees

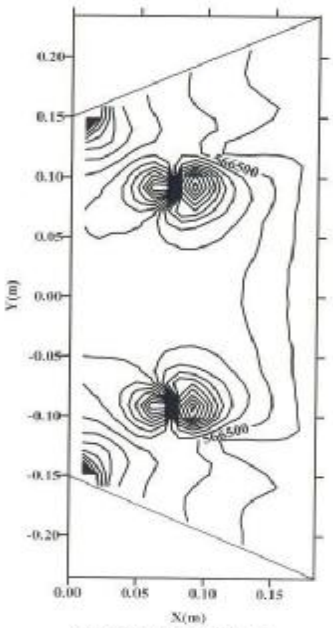

Fig. 14 : Pressure contours angle = 25 degrees, with snout

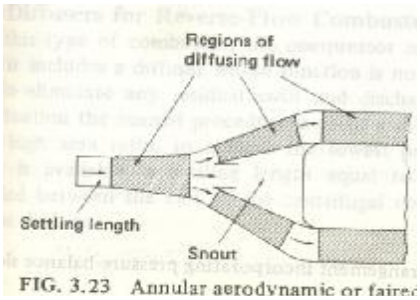

FIG. 3.23 Annular aerodynamic or faire

Fig. 15 Annular diffuser with snout [9]